HHS Public Access

Author manuscript

Anesthesiology. Author manuscript; available in PMC 2017 November 01.

Published in final edited form as:

Anesthesiology. 2016 November ; 125(5): 861–872. doi:10.1097/ALN.0000000000001322.

Neural Correlates of Sevoflurane-Induced Unconsciousness Identified by Simultaneous Functional Magnetic Resonance Imaging and Electroencephalography

Andreas Ranft, M.D.[2,*], **Daniel Golkowski, M.D.**[1,*], **Tobias Kiel, M.D.**[2], **Valentin Riedl, M.D., Ph.D.**[3], **Philipp Kohl**[2], **Guido Rohrer**[1], **Joachim Pientka**[2], **Sebastian Berger, M.Sc.**[2], **Alexander Thul**[1,2], **Max Maurer**[1,2], **Christine Preibisch, Ph.D.**[3], **Claus Zimmer, M.D.**[3], **George A. Mashour, M.D., Ph.D.**[4], **Eberhard F. Kochs, M.D.**[2], **Denis Jordan, Ph.D.**[2,#], and **Rüdiger Ilg, M.D.**[1,#]

[1]Department of Neurology, Klinikum rechts der Isar der Technischen Universität München, 81675 München, Germany

[2]Department of Anesthesiology, Klinikum rechts der Isar der Technischen Universität München, 81675 München, Germany

[3]Department of Neuroradiology, Klinikum rechts der Isar der Technischen Universität München, 81675 München, Germany

[4]Anesthesiology Department, University of Michigan Medical School, Ann Arbor, Michigan 48109, United States

Abstract

Background—The neural correlates of anesthetic-induced unconsciousness have yet to be fully elucidated. Sedative and anesthetic states induced by propofol have been studied extensively, consistently revealing a decrease of frontoparietal and thalamocortical connectivity. There is, however, less understanding of the effects of halogenated ethers on functional brain networks.

Methods—We recorded simultaneous resting-state functional magnetic resonance imaging (fMRI) and electroencephalography in 16 artificially ventilated volunteers during sevoflurane anesthesia at burst suppression, 3 volume % (vol%) and 2 vol% steady-state concentrations for 700 s each to assess functional connectivity changes compared to wakefulness. Electroencephalographic data were analyzed using symbolic transfer entropy (surrogate of information transfer) and permutation entropy (surrogate of cortical information processing).

Corresponding author (including raw data and study protocol): Daniel Golkowski, Department of Neurology, Klinikum rechts der Isar der Technischen Universität München, Ismaninger Straβe 22, 81675 München, Germany, Golkowski@lrz.tum.de, Tel. +498941407970.

*,#equal contribution

For Disclosure:

Patent pending (GAM, through the University of Michigan) on measures of directional connectivity for brain monitoring (Application No.: 13/804,706, Filed March 14, 2013, “System and Method to Assess Causal Signaling in the Brain during States of Consciousness”).

Patent pending (DJ and EFK, through the Technische Universität München): International Application Number: PCT/EP 2012/001794, International Filing Date: April 26, 2012; Priority Date: DE 10 2011 100 173.9 filed on May 5, 2011.

All other authors have no conflicts of interest.

fMRI data were analyzed by an independent components (ICA) and a region-of-interest-based (ROI-based) analysis.

Results—Electroencephalographic analysis showed a significant reduction of anterior-to-posterior symbolic transfer entropy and global permutation entropy. At 2 vol% sevoflurane concentrations, frontal and thalamic networks identified by ICA showed significantly reduced within-network connectivity. Primary sensory networks did not show a significant change. At burst suppression, all cortical networks showed significantly reduced functional connectivity. ROI-based thalamic connectivity at 2 vol% was significantly reduced to frontoparietal and posterior cingulate cortices but not to sensory areas.

Conclusions—Sevoflurane decreased frontal and thalamocortical connectivity. The changes in BOLD connectivity were consistent with reduced anterior-to-posterior directed connectivity and reduced cortical information processing. These data advance the understanding of sevoflurane-induced unconsciousness and contribute to a neural basis of electroencephalographic measures that hold promise for intraoperative anesthesia monitoring.

Introduction

General anesthetics have been in clinical use for almost 170 years but the mechanism by which they impair consciousness is incompletely understood. Rigorous studies of anesthetic-induced unconsciousness in humans have typically been conducted with the intravenous agent propofol. Studies using high-density electroencephalography in humans have identified anteriorization of coherent alpha oscillations,[1,2] characteristic phase-amplitude coupling changes,[2] and decreased frontoparietal connectivity[3] as electroencephalographic correlates of propofol-induced unconsciousness. Studies using using functional magnetic resonance imaging (fMRI) have identified diminished corticocortical[4,5] and corticosubcortical[6] connectivity as neural correlates of propofol-induced unconsciousness; a preferential interference of functional connectivity between higher-order thalamic nuclei and association cortex during propofol-induced unconsciousness has also been demonstrated.[7] Neural correlates of propofol-induced unconsciousness identified by simultaneous fMRI and electroencephalography have been explored more recently.[8,9] We have previously shown that functional disconnection between anterior and posterior brain structures as assessed by fMRI is associated with a reduction of frontal-to-parietal directed connectivity (DC) as measured by symbolic transfer entropy (STEn) and a reduction of frontal permutation entropy (PEn). These two electroencephalographic measures served as surrogates of the ability to process information in local (PEn) and widespread (STEn) cortical networks. In summary, consistent observations from different imaging modalities suggest that frontal and thalamocortical information processing might play a key role in the generation of consciousness and impairment of this processing might be an important neurophysiological mechanism of the action of general anesthetics.

Despite significant progress in understanding the basis of propofol-induced unconsciousness, the neural mechanisms of halogenated ethers in humans are less well understood. Sevoflurane is arguably the best representative of this drug class to study in humans since it can be well tolerated during mask induction, thus enabling a single-agent technique. A recent study using high-density electroencephalography in healthy volunteers

demonstrated that sevoflurane-induced unconsciousness was associated with a functional disconnection in the alpha bandwidth between anterior and posterior structures.[10] Consistent with this finding, a subsequent study of fMRI that meticulously controlled for head motion found functional disconnections in frontoparietal networks and a thalamocortical breakdown.[11] Positron emission tomography (PET) studies demonstrated the important role of thalamus during anesthesia in humans in terms of specifically reduced thalamic metabolism.[12–14] Pharmacological manipulation of the central medial thalamus could even reverse the effect of sevoflurane anesthesia in rodents.[15,16] Together, these results suggest a key role of the thalamus in unconsciousness induced by sevoflurane.

Thus far, there have been no reports of simultaneous fMRI and electroencephalography to bridge the gap from neural mechanisms to intraoperative monitoring strategies. Furthermore, investigations of sevoflurane have been limited by the number of participants and confounds such as head motion that possibly resulted from a lack of clinically relevant anesthetic concentrations.[11,17]

In this study of healthy volunteers, we took advantage of a simultaneous electroencephalography-fMRI protocol to test whether the modulation of network activity as assessed by fMRI is paralleled by corresponding changes of entropy-based surrogates of information transfer and information content in the electroencephalogram. We tested the hypothesis that, like propofol, sevoflurane would reduce frontal information processing (PEn) and disrupt frontoparietal connectivity, resulting in a decrease of frontal-to-parietal DC (as measured by STEn)

Material and Methods

Study Participants

The ethics committee of the medical school of the Technische Universität München (München, Germany) approved the present study, and the study protocol was in accordance with the Declaration of Helsinki. Volunteers were given detailed information about the protocol and risks, and written informed consent was obtained at least 48 hours before the experimental session; volunteers were reimbursed for their participation. Twenty healthy adult males aged 20–36 (mean 26) years were recruited by means of notices posted on campus and via personal contact. Prior to inclusion in the study, a medical history was taken to assess any previous neurological or psychiatric disorder, as well as other contraindications of the planned procedure (physical status other than American Society of Anesthesiologists (ASA) I, chronic intake of medication or drugs, hardness of hearing or deafness, absence of fluency in German, known or suspected disposition to malignant hyperthermia, acute hepatic porphyria, a history of halothane hepatitis, obesity with a body mass index > 30 kg/m^2, gastrointestinal disorders with a disposition for gastroesophageal regurgitation, known or suspected difficult airway, presence of metal implants). A focused physical examination was performed and a resting electrocardiogram was recorded. Experiments were conducted between June and December 2013.

Study Protocol

Sevoflurane concentrations were chosen so that burst suppression was reached in all participants (around 4.4 vol%) and that subjects tolerated artificial ventilation (reached at 2.0 vol%). We favored a fixed intermediate concentration of 3.0 vol% over individualized concentrations to make group comparisons feasible. At the beginning of the experiments, volunteers were supine on a couch outside the fMRI scanner room and 63-channel electroencephalogram was recorded with eyes closed for 10 minutes. Afterwards, the first combined electroencephalogram and fMRI measurement (700 s) was carried out in the magnetic resonance tomography scanner. Participants were in a resting state with eyes closed. By means of visual online analysis of the electroencephalogram, it was verified that volunteers did not fall asleep during this baseline recording. After inserting an intravenous catheter in a vein on the dorsum of the hand, sevoflurane in oxygen was administered via a tight fitting facemask using a fMRI-compatible anesthesia machine (Fabius Tiro, Dräger, Lübeck, Germany). Sevoflurane as well as O_2 and CO_2 were measured by the cardiorespiratory monitor (Datex AS/3, General Electric, Fairfield, US); standard American Society of Anesthesiologists monitoring was performed. An end-tidal sevoflurane concentration (etSev) of 0.4 vol% was administered for 5 minutes, then increased in a stepwise fashion by 0.2 vol% every 3 minutes until the participant was unconscious, as judged by loss of responsiveness (LOR) to the repeatedly spoken command “squeeze my hand” two consecutive times. Sevoflurane concentration was then increased to reach an end-tidal concentration of approximately 3 vol%.

When clinically indicated, ventilation was managed by the physician and a laryngeal mask suitable for fMRI (i-gel, Intersurgical, Wokingham, UK) was inserted. F_iO_2 was then set at 0.8 and mechanical ventilation was adjusted to maintain end-tidal CO_2 at a steady concentration of 33 ± 1.71 mmHg during BS, 34 ± 1.12 mmHg during 3 vol% and 33 ± 1.49 mmHg during 2 vol% (throughout this article mean ± standard deviation). Norepinephrine was given by continuous infusion (0.1 μg/kg*min ± 0.01 μg/kg*min) to maintain the mean arterial blood pressure close to baseline values (baseline 96 ± 9.36 mmHg, BS 88 ± 7.55 mmHg, 3 vol% 88 ± 8.4 mmHg, 2 vol% 89 ± 9.37 mmHg, follow-up 98 ± 9.41 mmHg). After insertion of the laryngeal mask airway, sevoflurane concentration was gradually increased until the electroencephalogram showed burst suppression with suppression periods of at least 1000 ms and about 50 % suppression on parallel EEG (reached at 4.34 ± 0.22 vol %,), which is characteristic of deep anesthesia.[18] At that point, another 700 s of electroencephalogram and fMRI were recorded (see fig. 1A). Twelve more minutes of data were acquired at steady etSev levels of 3 vol% and 2 vol% respectively, each after an equilibration time of 15 minutes.

In a final step, we reduced etSev to two times the concentration at LOR. Since under this condition, most of the subjects moved or did not tolerate the laryngeal mask any more, this stage was not included in the analysis. In order to monitor the subject’s recovery from anesthesia, the scanner table was slid out of the scanner and sevoflurane administration terminated. The volunteer was at that point manually ventilated until spontaneous ventilation returned and was regularly asked to squeeze the physician’s hand; recovery of responsiveness was noted as soon as the command was followed. The laryngeal mask was

removed as soon as the patient opened his mouth on command. 15 minutes after recovery of responsiveness, the Brice interview[19] was administered to assess for awareness during sevoflurane exposure; the interview was repeated on the phone the next day. After 45 minutes of recovery, another combined measurement of fMRI and electroencephalography was obtained in the resting state with eyes closed. When participants were alert, oriented, cooperative, and physiologically stable, they were taken home by a family member or a friend appointed in advance.

Electroencephalogram Data Acquisition

Simultaneous electroencephalographic-fMRI recordings were performed using an fMRI-compatible, 64-electrode cap with equidistantly arranged ring-type sintered nonmagnetic Ag/AgCl electrodes (Easycap, Herrsching, Germany) and two 32-channel, nonmagnetic, battery-operated electroencephalographic amplifiers (BrainAmp MR, Brain Products, Gilching, Germany). Electrode impedance was kept below 5 kΩ using an abrasive gel (Easycap, Herrsching, Germany). An interface unit (SyncBox, Brain Products) was additionally connected to the amplifiers to reduce timing-related errors in the fMRI artifact correction by synchronizing the clocks of the electroencephalographic amplifiers and the fMRI gradients. One of the 64 channels registered the electrocardiogram and was placed over the chest (left anterior axillary line). All signals were recorded at 5 kHz sampling rate (BrainVision Recorder, Brain Products). The electroencephalographic signal preprocessing analyses were performed using BrainVision Analyzer 2 (Brain Products). fMRI gradient artifacts in the electroencephalogram were averaged using a sliding window and subtracted from the electroencephalographic signals.[20] The cardioballistic artifacts caused by cardiomechanical electrode induction were removed using a template-detection method. The templates were based on the detected local maxima (R-peaks) and subtracted from the electroencephalogram using sliding windows of 21 epochs.[20] Finally, basic artifact rejection (sweeps with amplitudes exceeding 250 μV) and average referencing were performed.

Electroencephalographic PEn

PEn, a nonparametric time series measure, has been established to reliably separate wakefulness from unconsciousness.[21–23] PEn quantifies the regularity structure of the neighboring order of signal values in order to reflect information content of the signal as a surrogate of local cortical information processing.[9,24] Distortions of the electroencephalogram recordings in high static and radiofrequency electromagnetic fields of the magnetic resonance tomography scanner challenge reliability of the signal analysis. A key advantage of the nonparametric PEn over parametric analysis methods is its robustness against artifacts, signal distortions, and poorly known characteristics of the underlying dynamics, which makes this approach comparatively permissive regarding the specific selection of embedding parameters (dimension m, time lag l).[21,25] To obtain a direct comparison to the previous analysis of simultaneous electroencephalogram and fMRI during propofol-induced LOR[9] we used: $m = 5$ and $l = 5$, which is in line with the signal length criterion $m! < N$ and allows a sufficient deployment of trajectories within the state space of the electroencephalographic β-band during wakefulness and sevoflurane anesthesia.[9]

Electroencephalographic STEn

We largely follow the 2013 paper of our group and therefore refer to it for detailed formulas.[9] Briefly, STEn was introduced by Staniek et al[26] in 2008 and has the advantages to analyze amplitude orders instead of amplitude values. In contrast to PEn, STEn represents a surrogate measure of directed information flow between two electroencephalographic signals X and Y. STEn is expected to attain positive values for unidirectional coupling with X as the driver of Y and negative values for Y driving X. Since $STEn_{X\to Y}$, $STEn_{Y\to X} > 0$, a value STEn = 0 indicates balanced bidirectional coupling. STEn is less sensitive to the choice of specific embedding parameters than comparable parametric measures of directed mutual interaction.[26–30] As with PEn we used $m = 5$, $l = 5$, and a transfer delay $\delta = 7-12$ corresponding to 35–60 ms. Since STEn is computed in the time domain, a direct comparison to frequency-based signal analysis is not meaningful. Nevertheless, the applied settings result in a focus on information transfer in time scales within the electroencephalographic β-band, which is suspected to be relevant for long-range intercortical information exchange.[31,32] If not specified, STEn is used below as a common shortcut for the directionality index and for $STEn_{X\to Y}$, $STEn_{Y\to X}$. Computation of PEn and STEn was performed using Lab-VIEW 8.5 (National Instruments, Austin, TX), where the core algorithms of PEn and STEn were embedded in C.

fMRI Acquisition and Preprocessing

Data acquisition was carried out on a 3-Tesla whole-body magnetic resonance tomography scanner (Achieva Quasar Dual 3.0T 16CH, Amsterdam, Netherlands) with an eight-channel, phased-array head coil. The data were collected using a gradient echo planar imaging sequence (echo time = 30 ms, repetition time = 1.838 ms, flip angle = 75°, field of view = 220x220 mm^2 , matrix = 72x72, 32 slices, slice thickness = 3 mm, and 1 mm interslice gap; 700 seconds acquisition time, resulting in 350 volumes). Anatomy was acquired before the functional scan using a T1-weighted sequence and 1x1x1 mm voxel size.

Data were preprocessed using Statistical Parametric Mapping (SPM8, Wellcome Trust Centre for Neuroimaging, University of London, UK) and Data Processing Assistant for Resting-State fMRI (DPARSF, State Key Laboratory of Cognitive Neuroscience and Learning, Beijing Normal University, China).[33] Functional and T1-weighted images were first reoriented manually and realigned to the mean image of all functional images. Next, the first three time points were removed and slice timing was corrected. Functional images from all sessions and structural images were coregistered to the standard fMRI template implemented in SPM8 and resliced to 2x2x2 mm voxel size. Structural scans were not repeated for subsequent sessions. All images were resliced to 2x2x2 mm voxel size using 3rd degree spline interpolation and normalized to Montreal Neurological Institute (MNI) space. Functional images were smoothed using a 3x3x3 mm Gaussian kernel. Importantly, there were no relevant movement artifacts that required exclusion of data (see fig. 1B, compare to Palanca et al[11]). In fact, during sevoflurane anesthesia with laryngeal mask airway, participant movement was reduced compared with the waking state. One participant had a single movement artifact exceeding 11 mm, contaminating about 3 frames. Excluding the subject from the analysis resulted in no significant difference from the presented results. We therefore decided to include the participant in the final data analysis.

fMRI Independent Component Analysis and Region-of-Interest-based Analysis

All data analysis steps not implemented in SPM8 or GIFT toolbox were implemented in Matlab 2014b (Mathworks, Natick, MA). To study the effect of different sevoflurane concentrations on brain networks, independent component analysis (ICA) was carried out. We used the INFOMAX algorithm of GIFT Toolbox with an ICASSO and 20 repetitions searching for 75 different independent components (ICs) including data from 16 subjects from all 5 stages of anesthesia (baseline awake, burst suppression, 3 vol%, 2 vol% and follow-up).[34] ICs were identified with ICs from the literature.[20] Masks of different ICs were created from T-maps from all subjects taking into account $T > 3.197$ ($p < 0.001$, uncorrected) and binarized afterwards.

For the region-of-interest-based (ROI-based) analysis we chose regions from the coregistered HarvardOxford atlas. We then extracted a mean time course from each anatomic ROI and employed this time course as a regressor of interest in a general linear model in SPM together with the six movement parameters from the realignment procedure as nuisance regressors. Generated voxel-wise coefficients of the regressor of interest were transformed into T-maps and plotted with SPM ($p<0.001$, uncorrected, unless otherwise stated). Statistical testing was carried out using a one-way repeated measure ANOVA model for the 5 phases of our experiment (baseline awake, burst suppression, 3 vol%, 2 vol% and follow-up) as conditions. Significance levels are either reported on the voxel-level (uncorrected) or on the cluster-level with family-wise error correction (denoted p_{FWE}).

In order to ensure intact BOLD coherence during sevoflurane anesthesia[12] we calculated the average cortical BOLD signal in a grey matter mask with respect to burst onset on the simultaneously recorded electroencephalogram. Through this analysis we could demonstrate that the global grey matter BOLD signal leads to a plausible hemodynamic response function (fig. 1C).

Statistical Analysis

Electroencephalographic Measures—All statistical analyses were carried out in Matlab. p-values less than 0.05 were deemed significant. Sample size was based on previous experiments using propofol. The effects of sevoflurane on the PEn in frontal, parietal, temporal, and occipital electroencephalogram (changes of information content) such as on the STEn–based information flow in frontoparietal, frontotemporal, frontooccipital, parietotemporal, parietooccipital, and temporooccipital electroencephalogram (changes of directed connectivity) were of interest. Therefore, values of PEn and of STEn in frontal (18 electrodes corresponding to Fp1-FC6 according to the 10–20 scheme), central (11 electrodes, C5-CP4), parietal (14 electrodes, P11-PO8), temporal (12 electrodes, FT1-TP12), and occipital (8 electrodes, O9-I12) recordings on the electroencephalogram were averaged. Effect of anesthesia on both parameters over the whole time course was analyzed using a one-way repeated measure ANOVA. Sensitivity to discriminate between two different levels of anesthesia was analyzed using a two-sided t-test and Bonferroni-corrected for multiple testing. Both PEn and STEn measures led to the same results inside and outside of the MR-scanner (waking state, fig. 1D).

fMRI measures—Mean z-values from the ICA analysis were extracted subject-wise from all ICs and further analyzed visually using an errorbar plot and, statistically, using two-sided t-test between states and Bonferroni-corrected (fig. 1E).

Similarly, all voxel-wise analyses of thalamocortical connectivity were carried out using one-side one-sample t-test implemented in SPM8 ($p<0.001$, uncorrected). The same approach was used for group comparisons between different stages of anesthesia.

Results

Effects of Sevoflurane on Frontoparietal Interaction

Electroencephalographic Measures—All stages of sevoflurane anesthesia led to significant ($p < 0.05$, Bonferroni corrected) reduction of PEn values in all pooled electrodes, namely frontal, central, right and left temporal, parietal and occipital areas when compared to the waking state (see also fig. 2A). A one-way repeated measure ANOVA showed a significant modulation through sevoflurane concentration in frontal electrodes (fig. 2B), parietal electrodes, right temporal, central, occipital and left temporal electrodes (see fig. 1A, Supplementary Digital Content, for a figure showing PEn values in temporal, parietal and occipital regions). The PEn analysis also showed significant differences across states while the differences across regions were not significant.

It is noteworthy that PEn shows higher values during burst suppression when compared to 3vol%. This effect results from higher values during suppression than during non-suppression signals, which is a common issue for univariate electroencephalographic-based measures. [35,36]

In STEn analysis, sevoflurane-induced unconsciousness caused decreased connectivity in the frontal-to-posterior direction during the 2vol% and 3vol% condition ($p < 0.05$, Bonferroni corrected), whereas frontotemporal STEn was not changed significantly during 2vol% and decreased significantly during 3vol% and burst suppression (fig. 2C). An ANOVA analysis revealed a significant modulation through sevoflurane anesthesia between frontal and parietal electrodes (fig. 2D), parietal and temporal electrodes, frontal and occipital electrodes, parietal and occipital electrodes and frontal and temporal electrodes. Temporal and occipital electrodes were not significantly modulated. Unlike PEn, frontoparietal STEn values were lower during BS when compared to 3vol%, which were lower compared to 2vol % (both not significant). It is noteworthy that only the frontoparietal STEn was reversed by sevoflurane anesthesia (fig. 1B, see Supplementary Digital Content, for a figure showing STEn values between regions not shown in fig. 2D). Findings with PEn and STEn were congruent with previous findings during propofol-induced unconsciousness.[9]

fMRI measures—In order to analyze how different concentrations of sevoflurane affect relevant cortical networks we performed a group ICA ($n = 16$) employing the ICASSO algorithm (GIFT Toolbox V1.3) searching 75 different components in 20 repetitions. We found ICs that were stable across runs and that were consistent with ICs reported in the literature.[20] Visual inspection of T-maps of different ICs suggested that they were differentially affected by sevoflurane concentration. To quantify this impression we

extracted mean z-values of all 75 ICs and 5 levels of consciousness (baseline wake, BS, 3 vol% sevoflurane, 2 vol% sevoflurane, follow-up) and performed group level statistics (see table 1, Supplementary Digital Content, describing the most prominent ICs found with glass brain view, MNI coordinates, cluster sizes, and p-values). Based on our preceding study of propofol, we had an a priori hypothesis about a breakdown of frontoparietal and default mode networks during loss of consciousness but expected sensory networks to be less affected or even unchanged. We grouped the ICs according to this hypothesis. The number of participants allowed segmentation of frontoparietal networks into anterior and posterior divisions.

Frontal networks revealed a significant decrease during 2 vol%, namely in the left and right frontal parts of the frontoparietal networks (fig. 3A) and the anterior default mode network. To reflect the specificity of this observation we also analyzed neighboring networks. The salience network, for example, did not show a significant decrease.

Parietal networks, containing the posterior division of the frontoparietal attention system and the posterior part of default mode network, exhibited changes that differed from their anterior counterparts (fig. 3B). The left and right dorsal frontoparietal network showed a significant decrease only during BS. The posterior default mode network revealed a behavior with significant decrease only during BS and 3 vol% compared to the wakeful state, but not at 2 vol%. Sensory networks, namely the primary visual system showed a significant decrease during BS and 3 vol%, while the primary auditory system showed significant decreases only during BS (fig. 3C). In contrast, the thalamic network (fig. 3D) showed a significant decrease during all levels of anesthesia.

In order to further analyze these findings in an assumption-free way, we sorted all ICs with respect to their decrease during 2 vol% when compared to the waking state, assuming that networks with the most pronounced susceptibility to sevoflurane-induced loss of consciousness are the most functionally relevant. This approach also revealed that the most significant decrease could be seen in IC 31 (thalamic network), IC 48 (left anterior frontoparietal network), IC 53 (right anterior frontoparietal network) and 25 (dorsolateral prefrontal network). On the other hand, the most pronounced significant increase during 2 vol% could be seen in IC 33 (left auditory network), IC 3 (basal ganglia network), IC 8 (bilateral ventral hippocampus) and IC 23 (right auditory network). A complementary ANOVA analysis of all 75 networks yielded the same results. All findings presented here were consistent in bihemispheric networks.

Effects of Sevoflurane on thalamocortical connectivity

Based on observations of impaired thalamocortical functional connectivity during sevoflurane anesthesia in prior studies[7,11] and our observation of a significant reduction of mean z-values in the ICA analysis, we hypothesized a reduced connectivity between thalamus and frontal areas. Past animal experiments already suggested that projections of the central medial thalamus, with afferents from the brainstem, are involved in attention and arousal.[37–39] Pharmacological manipulation of the central medial thalamus could even reverse the effect of sevoflurane anesthesia in rodents.[15,16]

To further elucidate the effect of sevoflurane on thalamocortical interaction, we analyzed the thalamic connectivity in a ROI-based approach using a general linear model in SPM8. Left and right thalamic ROI, respectively, were taken from Harvard-Oxford atlas. Here we could demonstrate that thalamocortical interaction was widespread during the waking state but diminished during all states of anesthesia (see fig. 4A–D).

During burst suppression the thalamus was functionally disconnected from cortical areas. The top five clusters that significantly correlated to thalamic BOLD fluctuations projected outside of the brain and were thus regarded as noise (see table 2, Supplementary Digital Content, showing top 5 decreased clusters with p-values, cluster size, MNI coordinate and peak T-value). It is also noteworthy that the thalamic BOLD activity was not synchronized with the occurrence of bursts on the electroencephalogram (fig. 4B).

During 3 vol% (fig. 4B), the decrease of connectivity compared to the wakeful state was widespread including the thalamus itself, frontal areas, and the cerebellum. At 2 vol% sevoflurane, thalamic connectivity to mainly parietal, occipital and temporal areas could be seen (fig. 4B, left). The comparison of the 2 vol% state versus both waking states (fig. 4C) revealed a significant decrease in thalamic connectivity in the thalamus itself, left dorsolateral prefrontal cortex, right dorsolateral prefrontal cortex, posterior cingulate cortex and around the ipsi- and contralateral intraparietal sulcus. Medial prefrontal cortex did not show this significant reduction in thalamic connectivity either in the left- and right-sided thalamus analysis. Similarly, all other reported results were symmetrical. Also noteworthy is the fact that a significant decrease of connectivity of thalamus and primary sensory areas was not found.

These observations could be replicated by a voxel-wise one-way repeated measure ANOVA analyzing the difference between both wakeful states at baseline and recovery and all stages of anesthesia. The main effects were seen in the posterior cingulate cortex, the thalamus, and the left dorsolateral prefrontal cortex. The same effects could be seen in the right-sided thalamus. This was consistent with findings from the ICA analysis, which showed preserved or increased activity in primary sensory networks.

Discussion

The current study demonstrates that sevoflurane differentially affects various functional networks of the brain. Sevoflurane at 2 and 3 vol% levels leads to a more profound decrease of fMRI-based measures of functional connectivity in frontal networks, especially ventral parts of the frontoparietal attention networks and, to a lesser extent, anterior parts of the default network. At the same time, thalamocortical functional connectivity was significantly decreased in all stages of anesthesia. By contrast, primary sensory networks demonstrated increased functional connectivity during 2 vol% sevoflurane, with activation levels similar to the waking state in 3 vol% sevoflurane. Electroencephalographic analyses revealed the consistent findings of a pronounced decrease in surrogates of information processing (PEn) in frontal cortex and reversal of DC (STEn) between frontoparietal electrode pairs.

Frontoparietal Networks and Consciousness

In the past decade, fMRI studies of anesthetic-induced unconsciousness have focused predominantly on propofol,[5,6,9,40–43] with very few including concomitant electroencephalographic recordings.[9] Almost all studies consistently found that propofol-induced unconsciousness was associated with a breakdown of medial or lateral frontoparietal network connectivity,[5,6,9,40,41,43] reflected also by a reduction of frontal-to-parietal information-theoretic measures in electroencephalography.[9,28,44] In particular, the default mode network and frontoparietal attention network have attracted attention and impaired information exchange has been mainly attributed to these networks. Recent fMRI studies of sevoflurane anesthesia[11,40] and disorders of consciousness in brain-injured patients[5] have also reported diminished function of these networks. However, contradictory findings have been reported in the neuroimaging studies of sevoflurane.[45–47] Differential effects on anterior and posterior parts of both default mode and attention networks were not observed in the past.

The dorsolateral prefrontal cortex (IC 53/63/25) showed the greatest decrease in activation during 2 vol% of sevoflurane when compared to all other cortical networks identified via ICA, while the posterior parts of both networks did not show this behavior at all. This observation supports the assumption of a prominent role of the frontal cortex in consciousness in humans, either through perceptual or attentional mechanisms.

Past studies have reported an impairment of frontoparietal information-theoretic and other directed functional connectivity measures derived from electroencephalographic recordings during propofol-induced loss of consciousness.[9,28,44] Furthermore, diminished frontal-to-parietal symbolic transfer entropy during sevoflurane anesthesia has been described before with low-resolution electroencephalography.[28] Although the anesthetic protocol employed in the current study started with higher doses of sevoflurane, the findings are consistent with recent work demonstrating reduced frontal-to-parietal directed phase lag index (in the alpha bandwidth) during sevoflurane-induced unconsciousness at <1 vol% end-tidal concentration after slow up-titration.[48] Analysis of permutation entropy as a surrogate for information content[24] further supports our fMRI data by revealing a pronounced reduction in frontal electrodes. In summary, both our electrophysiological and neuroimaging results support the interpretation that frontal areas are differentially susceptible to sevoflurane, suggesting the interpretation that unconsciousness (of sensory information) might result from impaired top-down information access important for normal conscious perception.

The pronounced reduction of EEG based surrogates of information content in frontal cortex together with the concomitant changes of functional connectivity in frontal brain networks, holds promise for the future development of a neuroscientifically-informed strategy for real-time monitoring in the operating room.

Thalamocortical Connectivity during Sevoflurane-induced Unconsciousness

The role of the thalamus in anesthetic-induced unconsciousness has been extensively investigated[9,12,13] and several imaging studies have demonstrated a reduction of thalamic connectivity and metabolism associated during unconsciousness due to sedative-

hypnotics.[11,12,14] Not only has pharmacologic modulation of thalamic activity been associated with diminished consciousness, but also been shown to reverse anesthetic effects[15,16] and improve behavioral indices in patients with disorders of consciousness.[49] A common denominator of the thalamic role in consciousness is the attention to external stimuli and regulation of wakefulness. In the current study we observed that sevoflurane anesthesia was associated with a reduction of bilateral thalamic connectivity with the posterior cingulate cortex and the bilateral frontoparietal attention system, while functional connectivity between the thalamus and sensory cortices was not altered significantly. This supports the interpretation that decreased consciousness cannot be explained by a decreased thalamocortical feed-forward processing of sensory information alone but is probably due to decreased interaction of higher order frontal networks with posterior sensory networks. In past studies, sevoflurane anesthesia led to an especially marked inhibition of thalamic metabolism.[12] Our experimental design cannot distinguish among the possibilities that (1) sevoflurane inhibits thalamic activation, which inhibits interaction with the frontal cortex, (2) sevoflurane inhibits frontal activation, which inhibits interaction with the thalamus, or (3) some combination thereof. The observation that the thalamus showed no synchronous activation with cortical burst activity, offers some support for (1). However, the breadth of molecular targets of sevoflurane and their wide distribution in the brain[50–52] lends credibility to a combined set of effects; further work is clearly required.

Limitations

This study has numerous limitations. First, fMRI and electroencephalographic analyses of sevoflurane anesthesia started at higher concentrations (consistent with BS), followed by reduced concentrations (3 and 2 vol%). This introduces the possibility that observed neural changes were associated with sevoflurane drug effects unrelated to those required to induce loss of consciousness, rather than state-specific effects strictly associated with unconsciousness. It also introduces the possibility that findings at lower concentrations of sevoflurane merely reflect the inadequate recovery of a certain brain area (e.g., frontal cortex) from higher doses of anesthetic. However, the functional breakdown of frontoparietal functional connectivity[10] and frontal-to-parietal directed connectivity[48] has also been identified with slow titration of sevoflurane to achieve unconsciousness at <0.5 minimum alveolar concentration, supporting our interpretation of the current findings. Furthermore, analyses at lower concentrations were conducted after steady-state equilibration. Second, the initially high doses have implications for the cerebral blood flow-metabolism coupling that forms the physiological basis for functional neuroimaging. It is known that sevoflurane induces a dose-dependent increase of cerebral blood flow, despite its reduction in cerebral metabolism.[53] However, the differential effects of sevoflurane on functional brain networks of the same vascular territory—including preserved activity and connectivity of the posterior part of the default mode network—and the consistent findings with BOLD-independent electroencephalographic measures of information transfer suggest that this could not have been a major confound. Finally, all connectivity measures have limitations, especially when considering information transfer. We emphasize that the analyzed information-theoretic measures represent only a *surrogate* for true information exchange, which can occur on multiple scales in the brain not measurable with electroencephalography. Additionally, our

data analysis gives an averaged picture of functional connectivity during various sevoflurane concentrations and is not capable of detecting dynamic changes of connectivity. [54]

Conclusions

In conclusion, this is the first study reporting concomitant fMRI and electroencephalographic data during clinically relevant concentrations of sevoflurane in healthy volunteers. We found that sevoflurane preferentially affected functional connectivity of higher-order frontal brain regions both in fMRI and the electroencephalogram as well as corresponding thalamocortical connectivity. These findings have significant implications for the understanding of the underlying mechanisms of unconsciousness induced by sevoflurane (and possibly other halogenated ethers) as well as intraoperative monitoring of general anesthesia using frontal electroencephalography.

Supplementary Material

Refer to Web version on PubMed Central for supplementary material.

Acknowledgments

For Funding:

National Institutes of Health (Bethesda, Maryland), grant R01 GM098578 (to GAM)

References

1. Supp GG, Siegel M, Hipp JF, Engel AK. Cortical hypersynchrony predicts breakdown of sensory processing during loss of consciousness. Curr Biol. 2011; 21:1988–1993. [PubMed: 22100063]
2. Purdon PL, Pierce ET, Mukamel EA, Prerau MJ, Walsh JL, Wong KF, Salazar-Gomez AF, Harrell PG, Sampson AL, Cimenser A, Ching S, Kopell NJ, Tavares-Stoeckel C, Habeeb K, Merhar R, Brown EN. Electroencephalogram signatures of loss and recovery of consciousness from propofol. Proc Natl Acad Sci U S A. 2013; 110:E1142–E1151. [PubMed: 23487781]
3. Boly M, Moran R, Murphy M, Boveroux P, Bruno MA, Noirhomme Q, Ledoux D, Bonhomme V, Brichant JF, Tononi G, Laureys S, Friston K. Connectivity changes underlying spectral EEG changes during propofol-induced loss of consciousness. J Neurosci. 2012; 32:7082–7090. [PubMed: 22593076]
4. Schroter MS, Spoormaker VI, Schorer A, Wohlschlager A, Czisch M, Kochs EF, Zimmer C, Hemmer B, Schneider G, Jordan D, Ilg R. Spatiotemporal reconfiguration of large-scale brain functional networks during propofol-induced loss of consciousness. J Neurosci. 2012; 32:12832–12840. [PubMed: 22973006]
5. Boveroux P, Vanhaudenhuyse A, Bruno MA, Noirhomme Q, Lauwick S, Luxen A, Degueldre C, Plenevaux A, Schnakers C, Phillips C, Brichant JF, Bonhomme V, Maquet P, Greicius MD, Laureys S, Boly M. Breakdown of within- and between-network resting state functional magnetic resonance imaging connectivity during propofol-induced loss of consciousness. Anesthesiology. 2010; 113:1038–1053. [PubMed: 20885292]
6. Mhuircheartaigh RN, Rosenorn-Lanng D, Wise R, Jbabdi S, Rogers R, Tracey I. Cortical and subcortical connectivity changes during decreasing levels of consciousness in humans: a functional magnetic resonance imaging study using propofol. J Neurosci. 2010; 30:9095–9102. [PubMed: 20610743]
7. Liu X, Lauer KK, Ward BD, Li SJ, Hudetz AG. Differential effects of deep sedation with propofol on the specific and nonspecific thalamocortical systems: a functional magnetic resonance imaging study. Anesthesiology. 2013; 118:59–69. [PubMed: 23221862]

8. Ni Mhuircheartaigh R, Warnaby C, Rogers R, Jbabdi S, Tracey I. Slow-wave activity saturation and thalamocortical isolation during propofol anesthesia in humans. Sci Transl Med. 2013; 5:208ra148.
9. Jordan D, Ilg R, Riedl V, Schorer A, Grimberg S, Neufang S, Omerovic A, Berger S, Untergehrer G, Preibisch C, Schulz E, Schuster T, Schroter M, Spoormaker V, Zimmer C, Hemmer B, Wohlschlager A, Kochs EF, Schneider G. Simultaneous electroencephalographic and functional magnetic resonance imaging indicate impaired cortical top-down processing in association with anesthetic-induced unconsciousness. Anesthesiology. 2013; 119:1031–1042. [PubMed: 23969561]
10. Blain-Moraes S, Tarnal V, Vanini G, Alexander A, Rosen D, Shortal B, Janke E, Mashour GA. Neurophysiological correlates of sevoflurane-induced unconsciousness. Anesthesiology. 2015; 122:307–316. [PubMed: 25296108]
11. Palanca BJ, Mitra A, Larson-Prior L, Snyder AZ, Avidan MS, Raichle ME. Resting-state functional magnetic resonance imaging correlates of sevoflurane-induced unconsciousness. Anesthesiology. 2015; 123:346–356. [PubMed: 26057259]
12. Kaisti KK, Langsjo JW, Aalto S, Oikonen V, Sipila H, Teras M, Hinkka S, Metsahonkala L, Scheinin H. Effects of sevoflurane, propofol, and adjunct nitrous oxide on regional cerebral blood flow, oxygen consumption, and blood volume in humans. Anesthesiology. 2003; 99:603–613. [PubMed: 12960544]
13. Alkire MT, Haier RJ, Fallon JH. Toward a unified theory of narcosis: brain imaging evidence for a thalamocortical switch as the neurophysiologic basis of anesthetic-induced unconsciousness. Conscious Cogn. 2000; 9:370–386. [PubMed: 10993665]
14. White NS, Alkire MT. Impaired thalamocortical connectivity in humans during general-anesthetic-induced unconsciousness. Neuroimage. 2003; 19:402–411. [PubMed: 12814589]
15. Lioudyno MI, Birch AM, Tanaka BS, Sokolov Y, Goldin AL, Chandy KG, Hall JE, Alkire MT. Shaker-related potassium channels in the central medial nucleus of the thalamus are important molecular targets for arousal suppression by volatile general anesthetics. J Neurosci. 2013; 33:16310–16322. [PubMed: 24107962]
16. Alkire MT, McReynolds JR, Hahn EL, Trivedi AN. Thalamic microinjection of nicotine reverses sevoflurane-induced loss of righting reflex in the rat. Anesthesiology. 2007; 107:264–272. [PubMed: 17667571]
17. Peltier SJ, Kerssens C, Hamann SB, Sebel PS, Byas-Smith M, Hu X. Functional connectivity changes with concentration of sevoflurane anesthesia. Neuroreport. 2005; 16:285–288. [PubMed: 15706237]
18. Lewis LD, Ching S, Weiner VS, Peterfreund RA, Eskandar EN, Cash SS, Brown EN, Purdon PL. Local cortical dynamics of burst suppression in the anaesthetized brain. Brain. 2013; 136:2727–2737. [PubMed: 23887187]
19. Brice DD, Hetherington RR, Utting JE. A simple study of awareness and dreaming during anaesthesia. Br J Anaesth. 1970; 42:535–542. [PubMed: 5423844]
20. Allen EA, Erhardt EB, Damaraju E, Gruner W, Segall JM, Silva RF, Havlicek M, Rachakonda S, Fries J, Kalyanam R, Michael AM, Caprihan A, Turner JA, Eichele T, Adelsheim S, Bryan AD, Bustillo J, Clark VP, Feldstein Ewing SW, Filbey F, Ford CC, Hutchison K, Jung RE, Kiehl KA, Kodituwakku P, Komesu YM, Mayer AR, Pearlson GD, Phillips JP, Sadek JR, Stevens M, Teuscher U, Thoma RJ, Calhoun VD. A baseline for the multivariate comparison of resting-state networks. Front Syst Neurosci. 2011; 5:2. [PubMed: 21442040]
21. Jordan D, Stockmanns G, Kochs EF, Pilge S, Schneider G. Electroencephalographic order pattern analysis for the separation of consciousness and unconsciousness: an analysis of approximate entropy, permutation entropy, recurrence rate, and phase coupling of order recurrence plots. Anesthesiology. 2008; 109:1014–1022. [PubMed: 19034098]
22. Li D, Li X, Liang Z, Voss LJ, Sleigh JW. Multiscale permutation entropy analysis of EEG recordings during sevoflurane anesthesia. J Neural Eng. 2010; 7:046010. [PubMed: 20581428]
23. Olofsen E, Sleigh JW, Dahan A. Permutation entropy of the electroencephalogram: a measure of anaesthetic drug effect. Br J Anaesth. 2008; 101:810–821. [PubMed: 18852113]
24. Bandt C, Pompe B. Permutation entropy: a natural complexity measure for time series. Phys Rev Lett. 2002; 88:174102. [PubMed: 12005759]

25. Cao Y, Tung WW, Gao JB, Protopopescu VA, Hively LM. Detecting dynamical changes in time series using the permutation entropy. Phys Rev E Stat Nonlin Soft Matter Phys. 2004; 70:046217. [PubMed: 15600505]
26. Staniek M, Lehnertz K. Symbolic transfer entropy. Phys Rev Lett. 2008; 100:158101. [PubMed: 18518155]
27. Barrett AB, Murphy M, Bruno MA, Noirhomme Q, Boly M, Laureys S, Seth AK. Granger causality analysis of steady-state electroencephalographic signals during propofol-induced anaesthesia. PLoS One. 2012; 7:e29072. [PubMed: 22242156]
28. Ku SW, Lee U, Noh GJ, Jun IG, Mashour GA. Preferential inhibition of frontal-to-parietal feedback connectivity is a neurophysiologic correlate of general anesthesia in surgical patients. PLoS One. 2011; 6:e25155. [PubMed: 21998638]
29. Nicolaou N, Hourris S, Alexandrou P, Georgiou J. EEG-based automatic classification of 'awake' versus 'anesthetized' state in general anesthesia using Granger causality. PLoS One. 2012; 7:e33869. [PubMed: 22457797]
30. Schreiber T. Measuring information transfer. Phys Rev Lett. 2000; 85:461–464. [PubMed: 10991308]
31. Hipp JF, Engel AK, Siegel M. Oscillatory synchronization in large-scale cortical networks predicts perception. Neuron. 2011; 69:387–396. [PubMed: 21262474]
32. Wang XJ. Neurophysiological and computational principles of cortical rhythms in cognition. Physiol Rev. 2010; 90:1195–1268. [PubMed: 20664082]
33. Chao-Gan Y, Yu-Feng Z. DPARSF: A MATLAB Toolbox for "Pipeline" Data Analysis of Resting-State fMRI. Front Syst Neurosci. 2010; 4:13. [PubMed: 20577591]
34. Himberg J, Hyvarinen A, Esposito F. Validating the independent components of neuroimaging time series via clustering and visualization. Neuroimage. 2004; 22:1214–1222. [PubMed: 15219593]
35. Jantti V, Alahuhta S. Spectral entropy--what has it to do with anaesthesia, and the EEG? Br J Anaesth. 2004:93. 150-1; author reply 151-2. [PubMed: 14665560]
36. Schneider G, Jordan D, Schwarz G, Bischoff P, Kalkman CJ, Kuppe H, Rundshagen I, Omerovic A, Kreuzer M, Stockmanns G, Kochs EF. European Multicenter EAMSG, Research Group Knowledge-based Signal P. Monitoring depth of anesthesia utilizing a combination of electroencephalographic and standard measures. Anesthesiology. 2014; 120:819–828. [PubMed: 24694845]
37. Steriade M, Glenn LL. Neocortical and caudate projections of intralaminar thalamic neurons and their synaptic excitation from midbrain reticular core. J Neurophysiol. 1982; 48:352–371. [PubMed: 6288887]
38. Krout KE, Belzer RE, Loewy AD. Brainstem projections to midline and intralaminar thalamic nuclei of the rat. J Comp Neurol. 2002; 448:53–101. [PubMed: 12012375]
39. Glenn LL, Steriade M. Discharge rate and excitability of cortically projecting intralaminar thalamic neurons during waking and sleep states. J Neurosci. 1982; 2:1387–1404. [PubMed: 7119864]
40. Huang Z, Wang Z, Zhang J, Dai R, Wu J, Li Y, Liang W, Mao Y, Yang Z, Holland G, Zhang J, Northoff G. Altered temporal variance and neural synchronization of spontaneous brain activity in anesthesia. Hum Brain Mapp. 2014; 35:5368–5378. [PubMed: 24867379]
41. Monti MM, Lutkenhoff ES, Rubinov M, Boveroux P, Vanhaudenhuyse A, Gosseries O, Bruno MA, Noirhomme Q, Boly M, Laureys S. Dynamic change of global and local information processing in propofol-induced loss and recovery of consciousness. PLoS Comput Biol. 2013; 9:e1003271. [PubMed: 24146606]
42. Purdon PL, Pierce ET, Bonmassar G, Walsh J, Harrell PG, Kwo J, Deschler D, Barlow M, Merhar RC, Lamus C, Mullaly CM, Sullivan M, Maginnis S, Skoniecki D, Higgins HA, Brown EN. Simultaneous electroencephalography and functional magnetic resonance imaging of general anesthesia. Ann N Y Acad Sci. 2009; 1157:61–70. [PubMed: 19351356]
43. Schrouff J, Perlbarg V, Boly M, Marrelec G, Boveroux P, Vanhaudenhuyse A, Bruno MA, Laureys S, Phillips C, Pelegrini-Issac M, Maquet P, Benali H. Brain functional integration decreases during propofol-induced loss of consciousness. Neuroimage. 2011; 57:198–205. [PubMed: 21524704]

44. Lee U, Kim S, Noh GJ, Choi BM, Hwang E, Mashour GA. The directionality and functional organization of frontoparietal connectivity during consciousness and anesthesia in humans. Conscious Cogn. 2009; 18:1069–1078. [PubMed: 19443244]
45. Deshpande G, Kerssens C, Sebel PS, Hu X. Altered local coherence in the default mode network due to sevoflurane anesthesia. Brain Res. 2010; 1318:110–121. [PubMed: 20059988]
46. Martuzzi R, Ramani R, Qiu M, Rajeevan N, Constable RT. Functional connectivity and alterations in baseline brain state in humans. Neuroimage. 2010; 49:823–834. [PubMed: 19631277]
47. Martuzzi R, Ramani R, Qiu M, Shen X, Papademetris X, Constable RT. A whole-brain voxel based measure of intrinsic connectivity contrast reveals local changes in tissue connectivity with anesthetic without a priori assumptions on thresholds or regions of interest. Neuroimage. 2011; 58:1044–1050. [PubMed: 21763437]
48. Moon JY, Lee U, Blain-Moraes S, Mashour GA. General relationship of global topology, local dynamics, and directionality in large-scale brain networks. PLoS Comput Biol. 2015; 11:e1004225. [PubMed: 25874700]
49. Schiff ND, Giacino JT, Kalmar K, Victor JD, Baker K, Gerber M, Fritz B, Eisenberg B, Biondi T, O'Connor J, Kobylarz EJ, Farris S, Machado A, McCagg C, Plum F, Fins JJ, Rezai AR. Behavioural improvements with thalamic stimulation after severe traumatic brain injury. Nature. 2007; 448:600–603. [PubMed: 17671503]
50. Hapfelmeier G, Schneck H, Kochs E. Sevoflurane potentiates and blocks GABA-induced currents through recombinant alpha1beta2gamma2 GABAA receptors: implications for an enhanced GABAergic transmission. Eur J Anaesthesiol. 2001; 18:377–383. [PubMed: 11412290]
51. Rudolph U, Antkowiak B. Molecular and neuronal substrates for general anaesthetics. Nat Rev Neurosci. 2004; 5:709–720. [PubMed: 15322529]
52. Scheller M, Bufler J, Schneck H, Kochs E, Franke C. Isoflurane and sevoflurane interact with the nicotinic acetylcholine receptor channels in micromolar concentrations. Anesthesiology. 1997; 86:118–127. [PubMed: 9009947]
53. Kuroda Y, Murakami M, Tsuruta J, Murakawa T, Sakabe T. Preservation of the ration of cerebral blood flow/metabolic rate for oxygen during prolonged anesthesia with isoflurane, sevoflurane, and halothane in humans. Anesthesiology. 1996; 84:555–561. [PubMed: 8659783]
54. Barttfeld P, Uhrig L, Sitt JD, Sigman M, Jarraya B, Dehaene S. Signature of consciousness in the dynamics of resting-state brain activity. Proc Natl Acad Sci U S A. 2015; 112:887–892. [PubMed: 25561541]

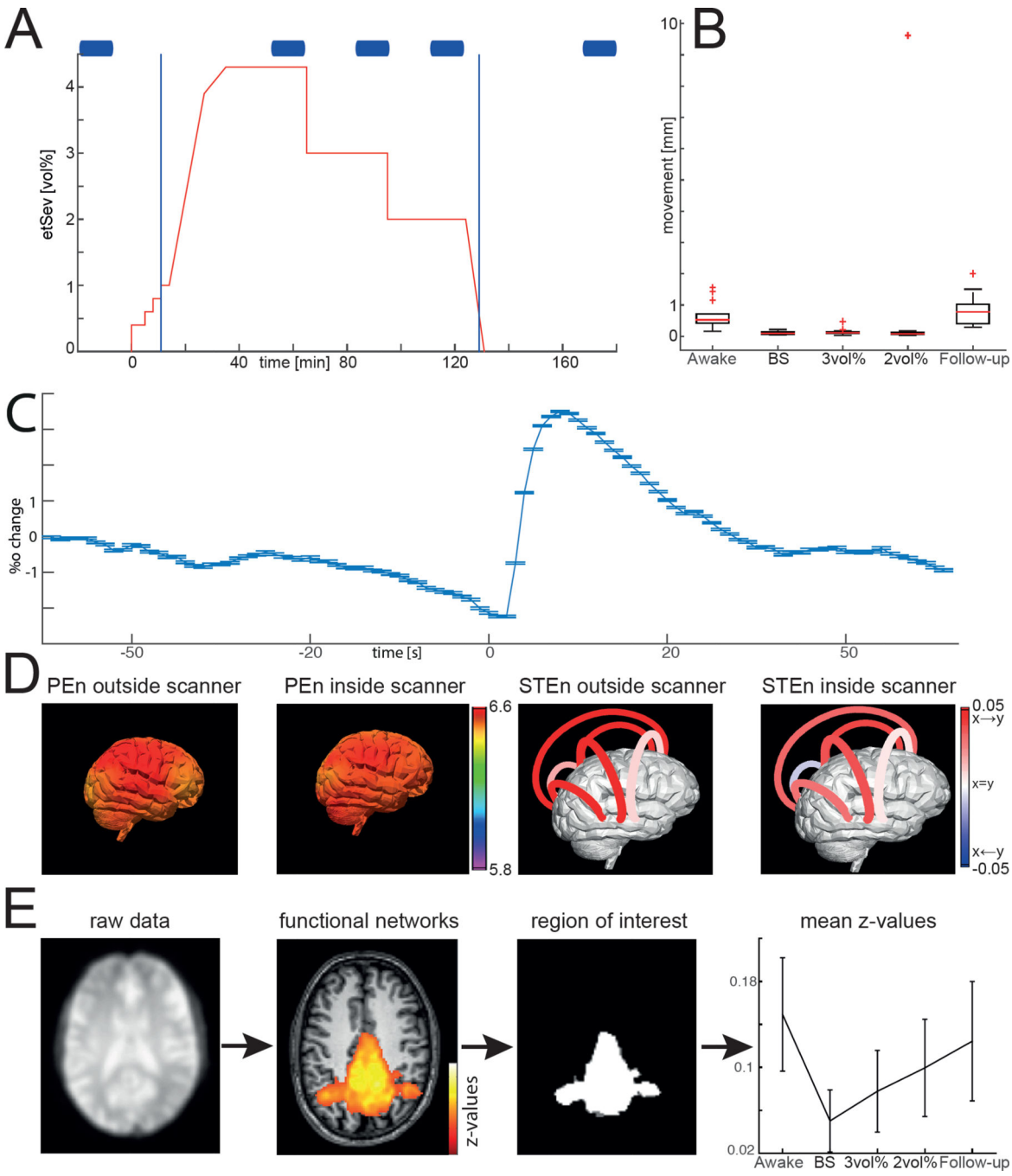

Fig. 1.

(A) Scheme of the experiment: The red trace displays sevoflurane concentration in the course of the experiment. Blue boxes represent 700 s of parallel functional magnetic resonance imaging and electroencephalography, vertical blue lines indicate loss and recovery of responsiveness. *(B)* Boxplots showing the maximum translation of each single subject across all phases of the experiment. Box represents 25th, 50th and 75th percentile. Whiskers correspond to +/− 2.7*standard deviation, outliers are denoted as +. *(C)* Average BOLD signal in a grey matter mask with respect to burst onset on parallel electroencephalogram

(mean ± standard error, 139 burst onsets in total). *(D)* Permutation entropy and Symbolic transfer entropy inside and outside the scanner projected on the cortical surface (x->y indicating i.e. frontal to parietal directed connectivity in frontoparietal electrode pairs). *(E)* Workflow of data analysis. Imaging data were realigned, normalized and smoothed, and then subdivided into 75 independent components (ICs) using an independent component analysis. Masks were generated through binarized maps employing voxel-wise one-sample t-tests (uncorrected, $p < 0.001$, SPM8). Mean z-values was calculated from the masks in each subject and given IC.

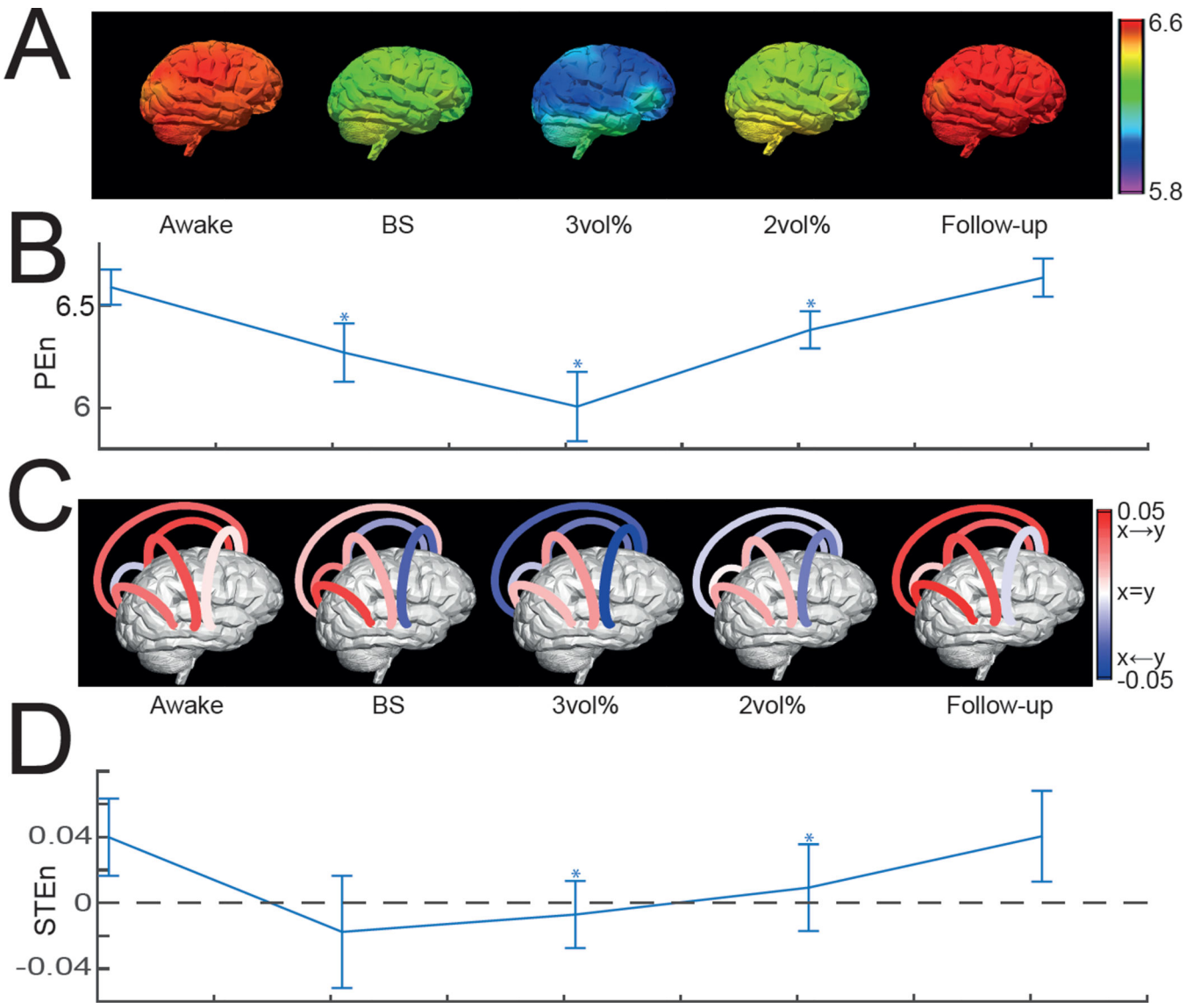

Fig. 2.

Electroencephalogram reveals decreased frontal information content and break down of frontoparietal information flow during anesthesia. *(A)* Information processing as represented by Permutation entropy (PEn) in different cortical regions rendered on a standard brain surface. *(B)* Plot of PEn (mean ± standard deviation) in pooled frontal electrodes. * marks significant decrease compared to wakeful state. *(C)* Directed connectivity represented by symbolic transfer entropy between frontal, parietal, temporal and occipital cortex. Color of loops encodes direction of information flow (e.g. with x->y indicating information flow from rostral to caudal, e.g. frontal to parietal directionality in frontoparietal connection). *(D)* Plot of frontoparietal information flow (Symbolic transfer entropy, mean ± standard deviation). * marks significant decrease compared to wakeful state.

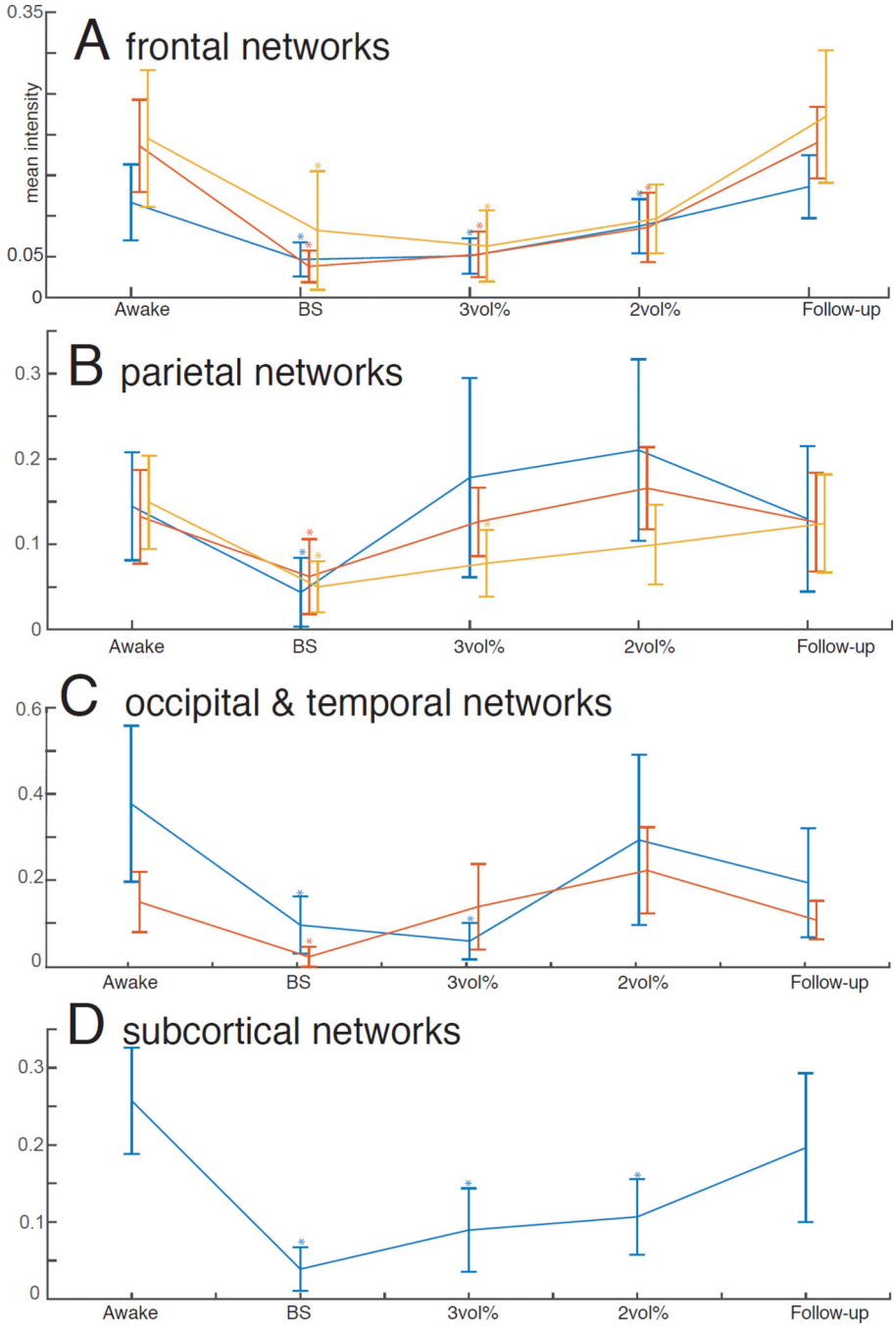

Fig. 3.

Functionally relevant networks exhibit distinct sensitivity to sevoflurane. (Average z-values from given mask are shown as group mean ± standard deviation; significant change compared to wakeful state is asterisked). *(A)* Frontal networks. Blue: IC48/left anterior frontoparietal network, red: IC53/right anterior frontoparietal network, yellow: IC63/anterior default mode network. *(B)* Parietal networks. Blue: IC42/left dorsal attention network, red: IC18/right dorsal attention network, yellow: IC37/posterior default mode network. *(C)*

Occipital and temporal networks. Blue: IC41/primary visual network, red: IC58/primary auditory network bilateral. (D) Subcortical networks: IC31/thalamic network.

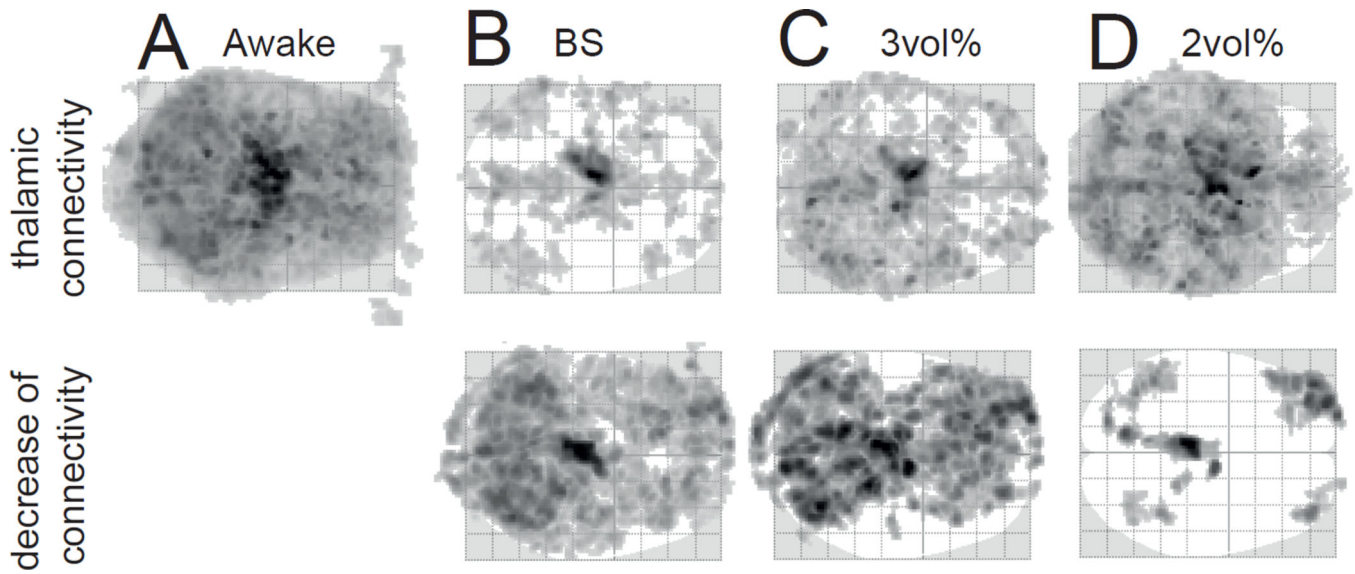

Fig. 4.

Reduced thalamocortical connectivity during sevoflurane anesthesia. *(A)* Region-of-interest (ROI) based analysis of the waking state with a seed ROI in the left thalamus of HarvardOxford Atlas showing widespread functional connectivity. Note: the top row shows ROI-based connectivity while the bottom row shows decrease compared to the wakeful state using contrasts of the factorial design (all voxel-wise one-sample t-test, uncorrected, $p < 0.001$, voxel threshold: 100, SPM8). *(B)* Functional connectivity of the thalamus during burst suppression and difference to wakeful state. *(C)* Functional connectivity of the thalamus during 3 vol% sevoflurane and difference to wakeful state. *(D)* Functional connectivity of the same seed ROI during 2vol% and difference to wakeful state.